Measurements of skin-friction fluctuations in turbulent boundary layers with miniaturized wall-hot-wires and hot-films

By Sebastian Bake[1] & Jens M. Österlund[2]

[1]Hermann-Föttinger-Institut für Strömungsmechanik, Technische Universität Berlin, Straße des 17. Juni 135, 106 23 Berlin, Germany
[2]Department of Mechanics, KTH, SE-100 44 Stockholm, Sweden

Submitted to *Phys. Fluids.*

Measurements of the fluctuating skin-friction are presented for turbulent boundary layers with zero pressure-gradient at high Reynolds numbers, using miniaturized wall-hot-wire and MEMS hot-film techniques. Results for quantities such as the turbulence intensity, skewness factor and flatness factor for the longitudinal skin-friction are presented and compared with findings from existing experiments. The experiments were carried out in the MTL-wind-tunnel at KTH in Stockholm and the LaWiKa wind-tunnel in Berlin at Reynolds numbers, based on momentum thickness θ, in the range $9800 < Re_\theta < 12400$.

1. Introduction

Detailed information about the fluctuating skin-friction is of basic importance for many types of flow and heat transfer problems and also for modeling purposes. A review of existing experiments were given by Alfredsson *et al.* (1988) and more recently on experimental techniques by Fernholz *et al.* (1996). The main difficulty is to design a skin-friction measurement technique with good dynamic response over the whole frequency range of interest and at the same time making the sensor size small enough to resolve the smallest scales in the turbulence. Most techniques such as the flush-mounted hot-film suffer from heat losses to the substrate which attenuates the response for high frequency fluctuations resulting in a difference between the static calibration and the dynamic response, e.g. a too low turbulence intensity

$$T_{\tau_w} = \frac{\sqrt{\overline{\tau_w^2}}}{\overline{\tau_w}} \tag{1}$$

is obtained.

The rapid development in the Micro-Electro-Mechanical-Systems (MEMS) area have resulted in new micro-machined hot-film sensors (Jiang *et al.* 1996)

	MTL	LaWiKa
test facility	flat plate	axisymmetric test section
length	7 m	6 m
width	1.2 m	$d = 0.41$m
temperature variations ΔT	< 0.05 °C	< 0.1 °C
free stream turbulence T_{U_∞}	0.02%	0.04%
max U_∞	69 m/s	34 m/s
probe position X	5.5 m	4.3 m

TABLE 1. Basic characteristics of the MTL and LaWiKa wind-tunnels in Stockholm and Berlin.

where the heat flux to the substrate is being reduced by placing the hot-film on a diaphragm on top of a vacuum cavity. Also the micro-machining technology allows for making very small hot-films to address the problem of spatial averaging.

Instead of using flush-mounted hot-films Alfredsson *et al.* (1988) used a hot-wire on the wall, that is elevated only a few μm from the wall to reduce the heat flux to the wall. This technique has been further developed by Fernholz *et al.* (1996) and a large effort has been put into the design and construction of miniaturized wall-hot-wire sensors for this type of experiment. The main purpose of this investigation is to determine statistical quantities of the skin-friction fluctuations in high Reynolds number turbulent boundary layers using current state-of-the-art hot-films and hot-wire-on-the-wall techniques.

2. The test facilities

Experimental results were obtained using two facilities, the MTL wind-tunnel at KTH and the LaWiKa wind tunnel at HFI. A brief description of the facilities and the experimental procedures are given below.

2.1. *The set-up at KTH*

Part of the experiments were carried out in the MTL-wind tunnel at the department of mechanics, KTH. The MTL-wind tunnel is specially designed to have good flow uniformity and low turbulence level. The temperature is controlled to within $\pm 0.05\,^{\circ}C$. The test section is 7 m long with a cross sectional area of 1 m^2 (1.2×0.8m^2). The top and bottom walls are adjustable in order to control the the streamwise velocity distribution in the test section. Special care have been taken to reduce acoustic noise and most of the walls have acoustic treatment. The velocity can be controlled between 0-69 m/s. For an overview of the basic properties of the MTL wind-tunnel see table 1. For a detailed description of the characteristics of the MTL wind-tunnel see Johansson (1992).

The boundary layer plate is a sandwich construction of aluminum sheet and aluminum square tubes and is divided into 7 sections and an adjustable flap that extends into the first diffuser, giving a total length of the set-up of about 8.7 m. The first section has an elliptical nose ($AR = 5$) fixed at the leading edge. Two pressure taps in the elliptical nose are used to position the stagnation point at the centerline of the plate. The positioning of the stagnation point is done by the flap. The plate is mounted in the tunnel resting on two longitudinal beams. It is positioned in a horizontal plane. By adjusting the position of the top and bottom walls of the tunnel the pressure gradient is minimized. The streamwise variation of the freestream velocity was less than 0.15% of the freestream velocity at the leading edge of the plate. The measurement section of the plate was equipped with two circular inserts, for instrumentation and a traversing system.

The normal transition of the laminar boundary layer occurs at a position several meters from the leading edge. To fix the transition close to the leading edge a trip was introduced. The trip was selected to give transition at the trip in the velocity range used in these experiments, and consisted of 8 rows of Dymo brand embossing tape with the letter "V". The two-dimensionality of the boundary layer was checked by measuring the spanwise variation of the friction velocity u_τ, and it was found to be less than $\pm 0.7\%$.

The mean wall-shear stress was determined by oil-film interferometry, see Fernholz *et al.* (1996) and Paper 8. The oil-film results was used to fit a logarithmic skin-friction-law of the type

$$c_f = 2\left[\frac{1}{\kappa}\ln(Re_\theta) + C\right]^{-2}, \tag{2}$$

with the resulting constants $\kappa = 0.384$ and $C = 4.08$. The skin friction variation was found to be in good agreement with other methods including the new near-wall method by Österlund and Johansson (Paper 8). The near-wall method utilizes direct measurement of the velocity profiles in the similarity region near the wall (the buffer region) but outside the region where hot-wire measurements in air are subjected to errors due to heat conduction to the wall. The profiles are then fitted to a universal profile obtained from DNS in the interval $6 < y^+ < 20$. Results from the oil-film interferometry are shown in figure 1 together with data from HFI and the skin friction correlation by Fernholz & Finley (1996).

The mean flow characteristics of the boundary layer showed a well defined logarithmic overlap region for Reynolds numbers (Re_θ) above 6000 and were reported in Österlund *et al.* (1999).

2.2. *The set-up at HFI*

The second part of the experiments was performed in the Laminar Wind Tunnel (LaWiKa) of the Hermann-Föttinger-Institute of Berlin Technical University. It is a closed-circuit tunnel with an axisymmetric test section made of Plexiglas

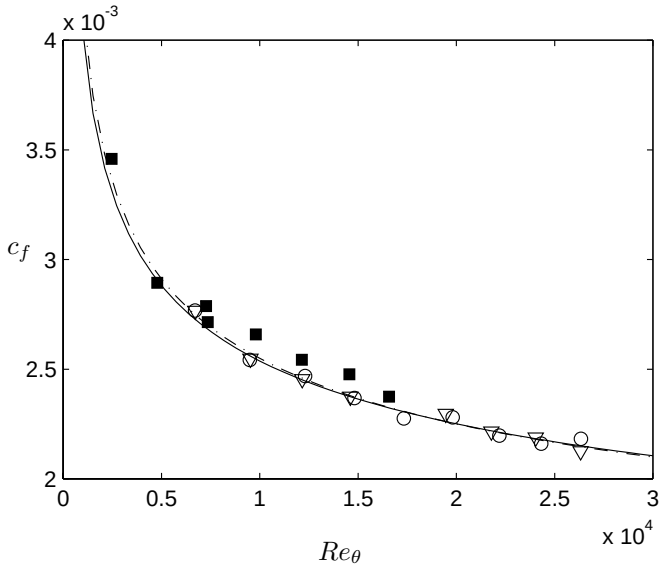

FIGURE 1. Skin-friction coefficient c_f. ∘ and ▽: KTH oil-film interferometry. –·–: best-fit of logarithmic friction law (equation 2) to the oil-film data. —: Skin-friction law from Fernholz & Finley (1996). ■: HFI Prestontube measurements.

tubes of various length with an inner diameter of 0.44 m and a total length of 6 m. It has a centrifugal fan and an additional blower to remove the nozzle boundary layer at the entry of the test section. To reduce the noise level in the wind tunnel the fan is mounted in a casing with sound attenuation. The bends are fitted with quarter circle turning vanes filled with mineral wool between perforated sheets. The test section has a sound muffler (quarter wave resonator) at the end to reduce the influence of fan-generated noise. In the settling chamber a non-woven filter mat and a single, precisely manufactured, perforated metal plate (64 % open area ratio) are used for damping of flow disturbances. The settling chamber is followed by a 2 m long axisymmetric nozzle with a 18:1 contraction ratio. The mean velocity distribution at the entry of the test section was uniform with a deviation from the mean $< 1\%$. The flow temperature can be controlled with a water cooler. For an overview of the basic characteristics of the LaWiKa see table 1. For a further description of the flow quality see Fernholz & Warnack (1998). The boundary-layer under investigation starts at the elliptic leading edge of the test section and develops downstream on its inner wall. It was tripped by means of a Velcro tape with a height of 3 mm situated 0.24 m downstream the leading edge. Because of the axisymmetric shape of the test section no corner-flow effects occur.

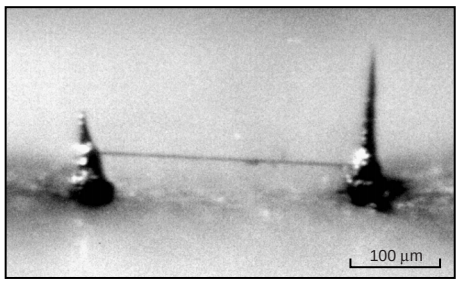

FIGURE 2. Photograph of a type 2 wall-hot-wire. Wire length 280μm, wire diameter 1.27μm and wire height above the wall 35μm.

For the probe insert a streamwise slot of 20 mm width was milled along one pipe section and filled with a series of interchangeable plugs. The Preston tubes, static taps and the wall hot-wires could be inserted in these plugs. For an optimal flush mounting the wall hot-wire probes were inserted under a microscope. The mean skin-friction values to calibrate the wall hot-wires were measured with Preston tubes (diameter between 1 and 2 mm) and are compared with the correlation by Fernholz & Finley (1996) in figure 1.

3. Sensor design

3.1. *Wall-hot-wires*

Three types of wall-hot-wire probe designs were used. The probe body of all types consists of a ceramic cylinder in a steel tube with 3 mm diameter. The ceramic isolates and holds the two prongs with the hot-wire. The first probe design was a wire elevated from the wall soldered onto two prongs with large separation. The wire ends were gold-plated to obtain a length to diameter ratio > 200 for the active part of the wire with a diameter of 2.5 μm.

The second type had prong tips thinned down to 35 μm and polished flush with the surface. The wire ends were fixed in two cones of solder plummet extending the prongs to the desired wire height, the active wire length now being the distance between the solder cones (see figure 2). The wires (diameter 1.27 and 0.64 μm) made of platinum-rhodium were not plated at the ends because of their mechanical infirmity.

The third and last type was designed like type two except that the wire was welded directly onto the prongs polished flush with the surface. This results in a slightly bent wire with an average height above the wall of only a few μm. This type was first used by Alfredsson *et al.* (1988).

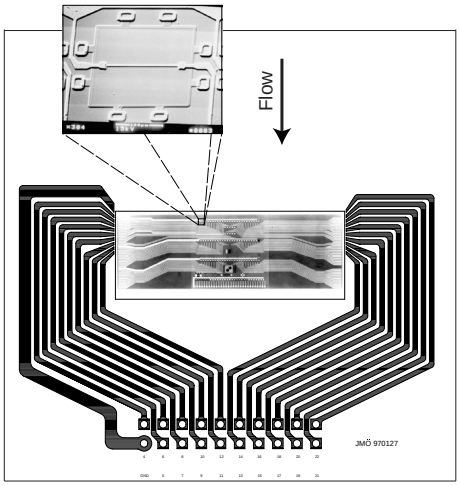

FIGURE 3. MEMS hot-film sensor chip from UCLA/Caltech (Jiang *et al.* 1996), mounted in the center of a printed circuit board providing the electrical connections. A blow-up of one of the vacuum insulated hot-films is also shown.

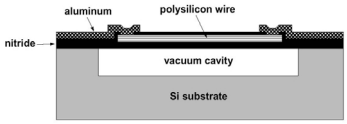

FIGURE 4. Cross-section, in a spanwise plane, of one hot-film sensor (Jiang *et al.* 1996).

3.2. *MEMS hot-film*

The MEMS hot-film used in the experiments at KTH was designed by the MEMS group at UCLA/Caltec (Jiang *et al.* 1996, 1997; Ho & Tai 1998). It was flush-mounted with a printed circuit board for electrical connections which in turn was flush-mounted into a Plexiglas plug fitting into the instrumentation insert of the measurement plate-section, see figure 3. The alignment was ensured by using a microscope during the mounting of the sensor set-up. The MEMS sensor chip was consisting of four rows of 25 sensors with a spanwise separation of 300 μm. The length of the poly silicon hot-film is 150μm and the width 3μm. It is placed on a 1.2μm thick silicon-nitride diaphragm with dimensions 200μm $\times$ 200μm. Thermal insulation of the hot-film to the substrate is provided by a 2μm deep vacuum cavity underneath the diaphragm, see figure 4. In this experiment only one of the hot-films was used.

4. Experimental procedure

The wall-hot-wire and the hot-film was calibrated in the turbulent boundary layer against the mean skin-friction obtained using oil-film interferometry or Preston tubes, here denoted τ_w^*. A Kings law modified for near-wall effects (Fernholz *et al.* 1996) was used to relate the anemometer output voltage E and the skin-friction τ_w,

$$\tau_w = \left(\sqrt{u + \frac{k_1}{4} - k_2} - \frac{k_1}{2} \right)^2 ; \qquad u = (\frac{1}{B}(E^2 - A))^{1/n} \tag{3}$$

where A, B, n, k_1 and k_2 are constants. The constants in equation 3 were determined minimizing the sum of the mean-square-error, for all calibration points, between the measured mean skin-friction τ_w^* and the mean value $\overline{\tau_w}$ obtained applying relation 3 to the anemometer voltage signal E

$$\min \left(\sum (\tau_w^* - \overline{\tau_w})^2 \right). \tag{4}$$

One example calibration is shown in figure 5. In the top half of the figure the measured mean skin-friction τ_w^* is shown against the mean anemometer voltages as circles. The stars represent the mean skin-friction values resulting from the calibration procedure of the wall-hot-wire or hot film. The dotted line is the resulting calibration function (equation 3), note that it does not need to go through the calibration circles since it is the sum of the squared distances between the stars and the circles that is minimized. In the bottom half of the figure the probability density for the anemometer voltage P_E is shown. The long tails of the probability density results in a required calibration interval for the mean skin-friction from 0.3 to 3 times the value of interest, to avoid extrapolation of the calibration function outside of the calibration limits (dashed lines in figure 5). No extrapolation was used.

5. Experimental results

An overview of the skin-friction experiments carried out in the MTL and LaWiKa wind-tunnels are compiled in table 2 where also symbols are introduced. The demand for a large calibration range restricts the investigation to essentially one Reynolds number for each set-up implying that no Reynolds number trends can be extracted from the present data.

In figure 6 results for the skin-friction intensity T_{τ_w} are presented, for all experiments performed in this investigation, against the active sensor length in viscous units. The data show a similar decrease in intensity for increasing probe dimensions as a result of spatial averaging (see *e.g.* Johansson & Alfredsson 1983; Ligrani & Bradshaw 1987). The limiting value of the turbulent intensity for small probe lengths is here found to be about 0.41. For comparison the

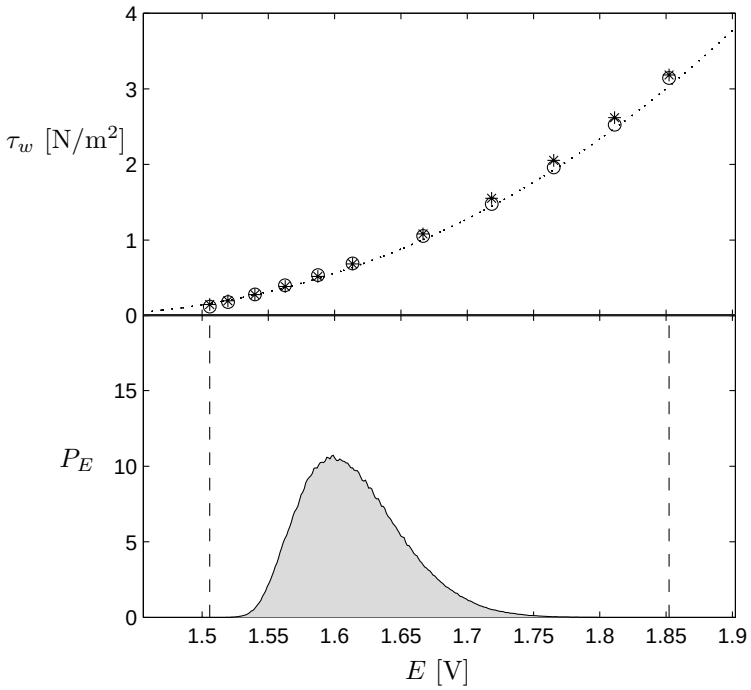

FIGURE 5. Calibration and measurement procedure. ○: Mean skin-friction from oil-film or Preston tube. ···: The fitted relation between anemometer voltage and skin-friction, equation 3. ∗: Mean skin-friction from hot-wire/hot-film calculated from the anemometer voltage signal using relation 3. -: Probability density function for the anemometer voltage signal (at $\overline{E} = 1.61$ V and $\overline{\tau_w} = 0.69\text{N/m}^2$).

results from the wall-hot-wire experiments at MIT in a turbulent boundary layer in air flow by Alfredsson *et al.* (1988) are also shown in figure 6 and show good agreement with the present data.The resulting intensity from the MEMS hot-film of 0.35 is more than 10% too low and can probably be attributed to remaining heat losses in the diaphragm that modifies the dynamic response compared to the static one. Still, the result represents a major improvement compared to previous findings using hot-films in air where values of about 0.1 are reported for the relative intensity of the wall shear stress fluctuations. Also, the rapid development in MEMS technology will probably lead towards large improvements in the near future. The wall-hot-wire of type 3, with the wire welded onto prongs flush with the wall, show a behavior similar to the hot-film. The plausible explanation being that heat flux from the wire, which is only a few μm above the wall, is partly absorbed by the wall and transferred

Symbol	Probe type	Re_θ	d [μm]	l [μm]	l/d	h [μm]	l^+	h^+	Facility
∘	WW1	12400	2.54	500	200	40	25	2	MTL
+	WW3	12400	1.27	200	160	5	10	0.25	MTL
×	MHF	12400	–	150	–	–	7.5	–	MTL
△	WW2	12400	1.27	200	160	35	12	1.2	MTL
•	WW1	9800	2.54	500	200	40	24	1.9	LaWiKa
▲	WW2	9800	1.27	200	160	40	10	1.9	LaWiKa
■	WW2	9800	1.27	280	220	35	13	1.7	LaWiKa
♦	WW2	9800	0.64	130	200	40	6.2	1.9	LaWiKa
▼	WW2	9800	0.64	140	220	40	6.7	1.9	LaWiKa

TABLE 2. Skin-friction measurements at KTH and HFI. WW: wall-hot-wire (number represents the type, see section 3.1). MHF: MEMS hot-film.

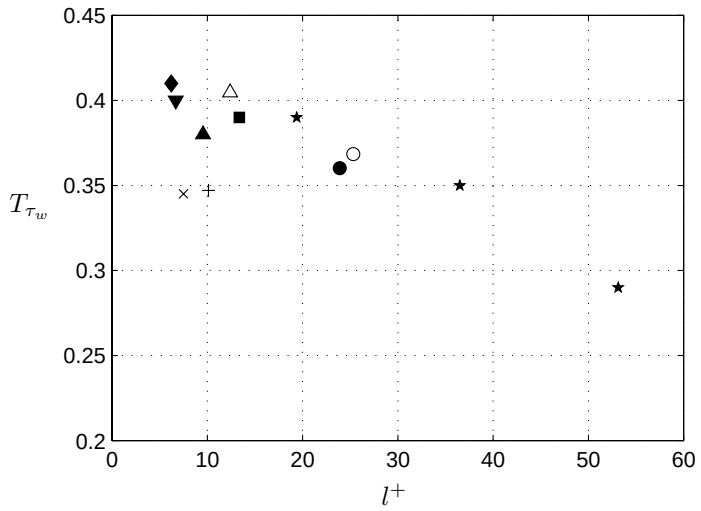

FIGURE 6. Turbulent skin friction intensity T_{τ_w}. For symbols, see table 2. ⋆: experiment by Alfredsson *et al.* (1988).

back to the fluid, in a mechanism similar to that for the hot-film. A connected issue is that the sensitivity of type 3 wall-hot-wires is very low due to damping resulting from the proximity of the wall.

Results for the Skewness and Flatness factors are presented in figure 7. No obvious trend, similar to the one found for the intensity, associated with the wire length is visible in the data and the values for the Skewness factor and

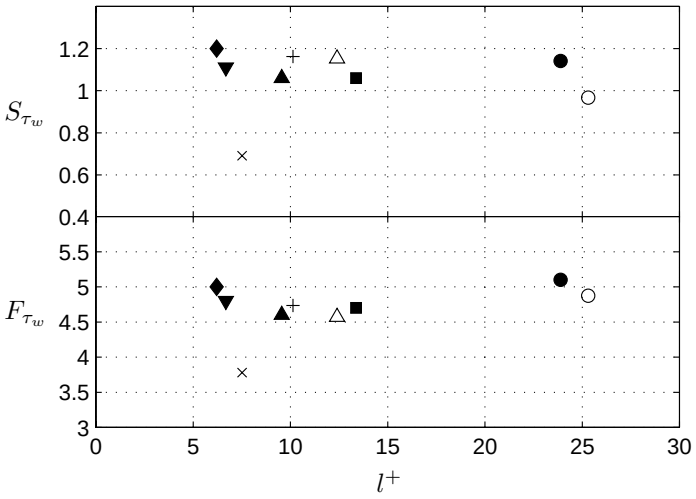

FIGURE 7. Skewness S_{τ_w} and Flatness F_{τ_w} factors for the fluctuating skin-friction. For symbols, see table 2.

for the Flatness factor are estimated as an average to be about 1.1 and 4.9, respectively. This is in good agreement with Alfredsson *et al.* (1988) who found the values 1.0 and 4.8.

6. Concluding Remarks

Based on the set of skin-friction measurements carried out using a variety of probe designs in two facilities it can be concluded that for Reynolds numbers of around 10,000 the streamwise fluctuating skin-friction intensity T_{τ_w} is close to 0.41. And that the values of the Skewness and Flatness factors are about 1.1 and 4.9, respectively.

The resulting skin-friction intensity from the MEMS type hot-film of 0.35 is a major improvement over existing types of hot-films with previously reported values of the fluctuating skin-friction intensity in air of about 0.1.The MEMS type hot-film and the wall-hot-wire of type 3, with the wire very close to the wall, both exhibits similar behavior and roughly 10% too low value for the fluctuating skin-friction intensity, it is believed to be a result of heat flux in the diaphragm, or in the wall-wire case heat flux to the wall, and back to the flow, resulting in a difference between static and dynamic responses.

7. Acknowledgments

The authors wish to thank Professor Chih-Ming Ho at UCLA for providing us with the MEMS hot-film probe. We wish to thank Mr. Ulf Landen and Mr. Marcus Gällstedt who helped with the manufacturing of the experimental set-up at KTH. Financial support from NUTEK and TFR for the KTH experiment is also gratefully acknowledged. We would like to thank Mr. Albrecht Ebner for exploring new dimensions while manufacturing the micro wall hot-wires at HFI. A visit to KTH in Stockholm was financed by the DAAD within a cooperation project between Sweden and Germany.

References

Alfredsson, P. H., Johansson, A. V., Haritonidis, J. H. & Eckelmann, H. 1988 The fluctuation wall-shear stress and the velocity field in the viscous sublayer. *Phys. Fluids A* **31**, 1026–33.

Fernholz, H. & Warnack, D. 1998 The effect of a favourable pressure gradient and of the Reynolds number on an incompressible axissymmetric turbulent boundary layer. Part 1. The turbulent boundary layer. *J. Fluid Mech.* **359**, 329–356.

Fernholz, H. H. & Finley, P. J. 1996 The incompressible zero-pressure-gradient turbulent boundary layer: An assessment of the data. *Prog. Aerospace Sci.* **32**, 245–311.

Fernholz, H. H., Janke, G., Schober, M., Wagner, P. M. & Warnack, D. 1996 New developments and applications of skin-friction measuring techniques. *Meas. Sci. Technol.* **7**, 1396–1409.

Ho, C.-M. & Tai, Y.-C. 1998 Micro-electro-mechanical-systems (MEMS) and fluid flows. *Ann. Rev. Fluid Mech.* **30**, 579–612.

Jiang, F., Tai, Y.-C., Gupta, B., Goodman, R., Tung, S., Huang, J. B. & Ho, C.-M. 1996 A surface-micromachined shear stress imager. In *1996 IEEE Micro Electro Mechanical Systems Workshop (MEMS '96)*, pp. 110–115.

Jiang, F., Tai, Y.-C., Walsh, K., Tsao, T., Lee, G. B. & Ho, C.-H. 1997 A flexible mems technology and its first application to shear stress sensor skin. In *1997 IEEE Micro Electro Mechanical Systems Workshop (MEMS '97)*, pp. 465–470.

Johansson, A. V. 1992 A low speed wind-tunnel with extreme flow quality - design and tests. In *Prog. ICAS congress 1992*, pp. 1603–1611. ICAS-92-3.8.1.

Johansson, A. V. & Alfredsson, P. H. 1983 Effects of imperfect spatial resolution on measurements of wall-bounded turbulent shear flows. *J. Fluid Mech.* **137**, 409–421.

Ligrani, P. M. & Bradshaw, P. 1987 Spatial resolution and measurement of turbulence in the viscous sublayer using subminiature hot-wire probes. *Experiments in Fluids* **5**, 407–417.

Österlund, J. M., Johansson, A. V., Nagib, H. M. & Hites, M. H. 1999 Wall shear stress measurements in high reynolds number boundary layers from two facilities. In *30th AIAA Fluid Dynamics Conference, Norfolk, VA*. AIAA paper 99-3814.